

# Electronic structure of dangling bonds in amorphous silicon studied via a density-matrix functional method

R. G. Hennig,\* P. A. Fedders, and A. E. Carlsson

*Department of Physics, Washington University, St. Louis, Missouri 63130*

(Received 21 June 2002; revised manuscript received 30 August 2002; published 21 November 2002)

A structural model of hydrogenated amorphous silicon containing an isolated dangling bond is used to investigate the effects of electron interactions on the electronic level splittings, localization of charge and spin, and fluctuations in charge and spin. These properties are calculated with a recently developed density-matrix correlation-energy functional applied to a generalized Anderson Hamiltonian, consisting of tight-binding one-electron terms parametrizing hydrogenated amorphous silicon plus a local interaction term. The energy level splittings approach an asymptotic value for large values of the electron-interaction parameter  $U$ , and for physically relevant values of  $U$  are in the range 0.3–0.5 eV. The electron spin is highly localized on the central orbital of the dangling bond while the charge is spread over a larger region surrounding the dangling bond site. These results are consistent with known experimental data and previous density-functional calculations. The spin fluctuations are quite different from those obtained with unrestricted Hartree-Fock theory.

DOI: 10.1103/PhysRevB.66.195213

PACS number(s): 71.55.Jv, 71.23.Cq, 71.15.Mb

## I. INTRODUCTION

Amorphous silicon ( $a$ -Si) inevitably contains dangling bonds which lead to electronically active defect states in the band gap. For undoped material, most dangling-bond states are singly occupied, and their spins provide a well defined experimental signature. The Fermi level is controlled by the energy of the gap states. Hydrogenation of  $a$ -Si reduces the density of defect gap states by passivating the dangling bonds and thus restores the band gap, making hydrogenated amorphous silicon ( $a$ -Si:H) applicable to solar cell devices.<sup>1</sup> However, even a small density of gap states can degrade performance, and gap states are also connected to degradation of device performance over time. Thus understanding the origin and properties of these states remains an important theoretical challenge.

The earliest theoretical work on defect states in  $a$ -Si and  $a$ -Si:H was based on tight-binding methods.<sup>2–7</sup> Biswas *et al.*<sup>3</sup> and Fedders and Carlsson<sup>4</sup> investigated the electronic structure of dangling and floating bonds in  $a$ -Si within tight-binding theory. They showed that the wave function of the gap defect states associated with the dangling bond is strongly localized on the threefold coordinated atom<sup>3</sup> and relatively independent of strain,<sup>4</sup> in contrast to the floating bond defect states. This difference was taken to imply that the electron-spin resonance (ESR) signal in  $a$ -Si:H arises from dangling bonds. In tight-binding calculations without electron-electron interaction terms, the localization of the spin of the gap states is the same as that of the charge density, since the remaining occupied states do not adjust to the electron charge in the dangling-bond gap state. This leads, in general to an overestimate of the charge density associated with the gap state. More recently, density-functional calculations of dangling-bond states using the local-density approximation have been performed.<sup>8</sup> They yield a charge localization of less than 15% on the central atom. This finding at first appeared to be at variance with ESR experiments, which showed that over 50% of the spin density of the energy gap

state is located on the central atom of the dangling bond.<sup>9,10</sup> However, recent calculations using the local spin-density approximation have shown that the degree of localization of the spin density is quite different from that of the charge density.<sup>11</sup> The energy cost to localize the charge density is substantially larger than the energy to localize the spin density.<sup>8,11</sup> This demonstrates the importance of correlation effects for a correct description of the electronic structure of the dangling bond, since in purely one-electron descriptions the charge and spin densities for a defect orbital are equivalent.

Because of these correlation effects, the extent of the applicability of current implementations of density-functional theory to the electronic properties of defects in  $a$ -Si:H is not clear. These implementations break down in the limit of strong correlations. In addition, current density-functional codes do not provide information on the spin and charge fluctuations at the defect. For this reason, it is useful to study the defect states with a method that is valid in the limit of strong interactions, and that provides information on electronic fluctuations. In this work a recently developed method based on density-matrix functional theory, developed for isolated strongly interacting orbitals,<sup>12</sup> is applied to the problem of a single dangling bond in  $a$ -Si:H. So far this method has only been applied to idealized models. In this paper we demonstrate that the method can be used to calculate the electronic structure of a semiquantitatively accurate model such as that treated here. Our results for the charge and spin distributions of the defect states are consistent with earlier results. We also make predictions for the fluctuations of the spin and charge.

The article is structured as follows. Section II describes the atomic structure of the model for  $a$ -Si:H. Section III introduces the Hamiltonian and describes the density-matrix functional used to calculate the ground state energy of the system. Section IV is the core of the paper, presenting our results for the electronic structure of the dangling bond. The effects of electron correlations on the energy of the defect state in the band gap are determined by comparison of results

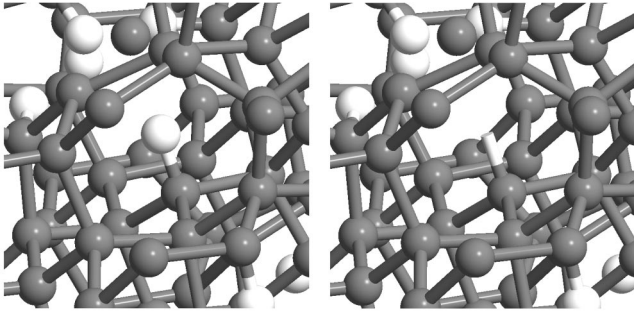


FIG. 1. Structure of *a*-Si:H around the dangling bond site. In the left panel, the hydrogen in the center bonds to a Si atom, whereas in the right panel the hydrogen atom is removed producing a dangling bond. For clarity, the relaxations of the structure due to the removal of the hydrogen atom are not shown.

from the density-matrix functional and the Hartree-Fock approximation in Sec. IV B. Charge and spin localization and fluctuations are discussed in Sec. IV C. The results are compared to density-functional calculations and experiments in Sec. IV D.

## II. STRUCTURE MODEL OF HYDROGENATED AMORPHOUS SILICON

The atomic model for amorphous hydrogenated silicon used here was employed in an earlier density-functional theory calculation.<sup>13</sup> It contains 122 Si atoms and 20 hydrogen atoms per fcc unit cell, with periodic boundary conditions. The atomic positions were obtained by doubling a previous, smaller unit cell, and subsequently annealing the structure. The edge length of the fcc cell is 11 Å. The hydrogen concentration of 14% is somewhat higher than what is commonly used in experimental samples ( $c \approx 10\%$ ). All hydrogen atoms are attached to the dangling bonds present in the structure, and each dangling bond is terminated by a hydrogen atom.

To create a single dangling bond in the model of amorphous hydrogenated silicon, hydrogen atom number 142 was removed from silicon atom 108 and the structure was relaxed using a density-functional approach.<sup>13</sup> Figure 1 shows the atomic structure surrounding the dangling bond site. The orientation of the dangling bond is roughly in the [111] direction. This particular dangling bond orbital was chosen since it is a typical realization of an isolated dangling bond surrounded by silicon atoms only, with hydrogen atoms farther away. The closest hydrogen atom is 4.3 Å away from the threefold coordinated Si atom, significantly further than the typical Si-H bond length of roughly 1.5 Å. The three nearest neighbor Si atoms are 2.4 Å away and the bond-angles range from 104° to 119°, typical values for *a*-Si:H.

## III. HAMILTONIAN AND METHOD OF SOLUTION

The electronic structure of the system is treated with a discrete Anderson-type Hamiltonian:

$$\mathcal{H} = \sum_{ij\sigma} h_{ij} c_{i\sigma}^\dagger c_{j\sigma} + U[n_{0\uparrow} n_{0\downarrow} - (n_{0\uparrow} + n_{0\downarrow})/2], \quad (1)$$

where  $i$  and  $j$  are orbital indices,  $\sigma$  denotes the spin and the dangling bond is orbital 0;  $c_{i\sigma}^\dagger$ ,  $c_{j\sigma}$ , and  $n_{0\sigma}$  are the usual second-quantized creation, annihilation, and number operators. In the one-electron part of  $\mathcal{H}$  the matrix elements  $h_{ij}$  include on-site energy terms and interatomic hopping terms. We restrict the interaction terms to the dangling-bond orbital because this orbital will have the greatest fluctuations in occupancy and will therefore be the most affected by the interactions. The correction in these terms proportional to  $(n_{0\uparrow} + n_{0\downarrow})/2$  compensates approximately for the neglect of interaction terms on the other orbitals. If these interaction terms were included, and treated at the Hartree-Fock level assuming half occupancy and no spin-polarization of the non-dangling-bond orbitals, the resulting Hamiltonian would have the non-dangling-bond orbital energies shifted upward by  $U(n_{0\uparrow} + n_{0\downarrow})/2$ ; we instead choose to simplify the Hamiltonian by shifting the dangling-bond orbital energy down. The Hamiltonian may thus be viewed as treating the interaction terms on the non-dangling-bond orbitals in an approximation to the Hartree-Fock approach.

The angular dependences of the one-electron terms are given by the Slater-Koster parametrization.<sup>14</sup> The Slater-Koster parameters are scaled with the interatomic distance,  $d$ , as  $1/d^2$ . There are several tight-binding parametrizations in the literature for Si-H.<sup>2,7</sup> Knief and Niessen compared different tight-binding parameter sets for *a*-Si:H to the experimental density of states.<sup>6</sup> For *a*-Si:H they found a better agreement with experimental results for the parameter set from Allan and Mele<sup>2</sup> than for the tight-binding parametrization by Min *et al.*<sup>7</sup> Both parametrizations use orthogonal basis functions with a minimal basis set of  $s$  and  $p$  valence orbitals, and include nearest neighbor interactions only. In the following, the parametrization by Allan and Mele is used.

The interactions of the up and down spin electrons of the dangling-bond orbital, described by the second term in  $\mathcal{H}$ , were treated using a recently developed density-matrix functional method.<sup>12</sup> This approach treats correlations by including multiconfiguration effects in an approximate fashion. In previous tests for model systems involving a single pair of interacting orbitals<sup>12</sup> it was shown to give accurate results for several electronic properties for weak, intermediate, and strong electron-electron interactions. In the density-matrix functional method the ground state energy,  $\langle \mathcal{H} \rangle$ , is approximated by a functional of the one-body density matrix,  $\hat{\rho}$ , defined by  $\rho_{ij\sigma} = \langle c_{i\sigma}^\dagger c_{j\sigma} \rangle$ . The expectation value of the one-electron part of the Hamiltonian is given exactly as a simple functional of the density matrix. The expectation value of the interaction energy,

$$E_{\text{int}} = U \langle n_{0\uparrow} n_{0\downarrow} \rangle, \quad (2)$$

is rigorously given as a functional of the local moments of the one-body density matrix projected on site 0.<sup>12</sup> The exact form of this functional is not known. However, for systems with only two interacting orbitals, such as that studied here, a lower bound for the interaction energy holds which is given in terms of the second moment of the density matrix:

$$U \sqrt{\sum_{\alpha \neq 0\uparrow, 0\downarrow} \rho_{0\uparrow, \alpha}^2} \leq \sqrt{(Un_{0\uparrow} - E_{\text{int}})(U(1 - n_{0\uparrow} - n_{0\downarrow}) + E_{\text{int}})} + \sqrt{E_{\text{int}}(Un_{0\downarrow} - E_{\text{int}})}. \quad (3)$$

A parallel result is obtained by switching up and down spins in the above inequality. In the ‘‘second-moment approximation’’ that we employ here, the interaction energy is obtained as a function of  $\hat{\rho}$  by replacing the inequality by an equality if this gives a positive value for the interaction energy; if not, the interaction energy is taken to be zero.

The density matrix of the model system is taken to be that which minimizes the total energy, subject to the constraint that all of its eigenvalues must be between zero and unity. This approach gives the correct density matrix for an exact density-matrix functional<sup>15</sup> and is the appropriate avenue to use with our approximate functional. The resulting density matrix, unlike those obtained from density-functional calculations, has a range of eigenvalues between zero and one and is thus not idempotent (for  $U \neq 0$ ). This is the correct behavior for interacting systems. The procedure for obtaining the energy-minimizing density matrix involves a constrained conjugate-gradient method described in more detail in Ref. 12. The computer time required for the minimization is  $\mathcal{O}(N^3)$ , where  $N$  is the number of orbitals.

## IV. ELECTRONIC STRUCTURE

### A. Without interactions

Electronic densities of states of the model of the completely hydrogenated amorphous silicon structure with  $U = 0$  were calculated using standard Brillouin-zone integration techniques using a  $5 \times 5 \times 5$  k-point mesh.<sup>16</sup> The hydrogen passivates the dangling bonds and gives a well-defined gap of about 1.2 eV. Compared to experimental values of the energy gap of 1.4 to 2.0 eV, the tight-binding parametrization<sup>2</sup> that we use underestimates the gap. However, the density of states of our model of amorphous hydrogenated silicon compares well to the density of states for larger models such as the ones investigated by Holender and Morgan using the same tight-binding parametrization.<sup>5</sup>

In the single dangling-bond electronic-structure calculations, the one-body part of the Hamiltonian was transformed via the recursion method<sup>17</sup> to a chain Hamiltonian of length 80. Because the recursion steps quickly left the original unit cell, the cell was replicated periodically. The starting point for the recursion procedure was an  $sp^3$  hybrid orbital with the orientation of the above dangling bond orbital (see Sec. II). The chain was truncated at level 80 with no terminator.

As a check on the accuracy of the recursion procedure, we obtain the electronic structure of  $a$ -Si:H with the dangling bond using both diagonalization of the chain Hamiltonian and standard Brillouin-zone integration techniques. Figure 2 shows the density of states from the Brillouin-zone integration. The recursion method obtains a band gap of 1.4 eV, in comparison to 1.3 eV for the BZ method. The satisfactory agreement between these results indicates that the recursion chain is sufficiently long for an accurate description of the electronic structure. Thus finite-size effects appear to be

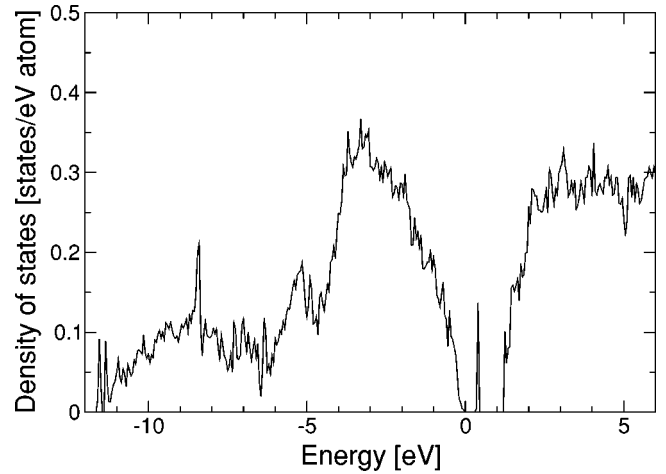


FIG. 2. Electronic density of states of  $a$ -Si:H containing an isolated dangling bond calculated by Brillouin-zone integration. The dangling bond leads to a defect state in the band gap.

small. (The band gaps are different from those in the absence of the dangling bond because of the atomic relaxations and the finite size of the supercell). The dangling-bond gap state is found to be 73% localized on the dangling-bond orbital. The energy is 0.4 eV above the valence band edge and 0.9 eV below the conduction band edge.

### B. Effects of interactions on gap state energies

To calculate the effects of interactions on the dangling-bond states, we apply the second-moment density-matrix algorithm described above to our Hamiltonian transformed into the chain representation. For comparison, we include results obtained by the unrestricted Hartree-Fock (UHF) method.

The second-moment method as described above gives the total energy for a fixed number of electrons, but not directly the defect energy levels. In an interacting electron system, a defect energy level is defined as a value of the chemical potential  $\mu$  at which the number of electrons in the system changes abruptly. Minimizing the thermodynamic potential  $E(N) - \mu N$  (at zero temperature), one readily shows that the number of electrons changes from  $N$  to  $N + 1$  when

$$\mu = E(N + 1) - E(N), \quad (4)$$

which is taken to be the gap state energy. The valence and conduction-band edges are defined in a similar fashion (they are discrete states because our chain has finite length).

Figure 3 shows the gap energy levels and band edges obtained in this fashion as functions of the interaction energy,  $U$ , for the second-moment and the UHF approximations. We first note that the conduction and valence-band edges depend only weakly on the Coulomb repulsion on the dangling bond, as the gap is mostly determined by the non-interacting tight-binding part of the Hamiltonian. The energy of the gap states in the second-moment approximation varies roughly linearly with  $U$ , for small  $U$ , as expected on the basis of first-order perturbation theory. At larger values of  $U$ , beyond about 3 eV, the splitting approaches a finite limit. The

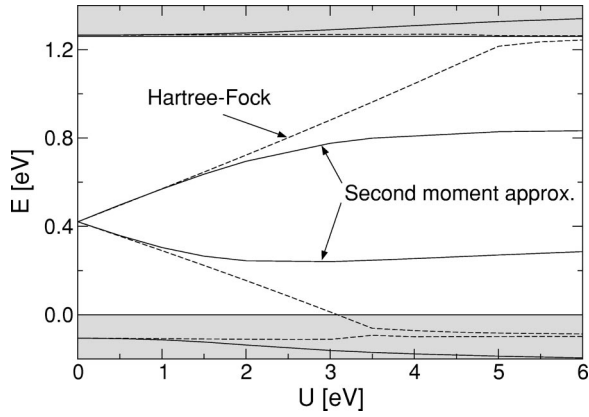


FIG. 3. Energy levels of dangling-bond defect states in the band gap as a function of the interaction energy  $U$ . The energy levels are given relative to the valence band edge obtained with the BZ integration method for  $U=0$ .

UHF results are in agreement with the second-moment results up to about  $U=2$  eV, but the levels continue to split linearly with energy until they merge with the valence and conduction bands. On the basis of exact diagonalization many-body calculations for small clusters including only the nearest few orbitals,<sup>18</sup> we feel that the behavior of the second-moment approximation is correct. In the diagonalization calculations we find that it is possible to add a second electron to the gap states without an energy increase proportional to  $U$ , because the inclusion of correlation effects allows the electrons to avoid both being in orbital 0 at the same time.

### C. Spin and charge on dangling-bond site

The permanent spin on the dangling-bond site is obtained directly in terms of the appropriate elements of the density matrix:

$$\langle s_0 \rangle = \langle n_{0\uparrow} - n_{0\downarrow} \rangle. \quad (5)$$

Figure 4 shows the dependence of this spin on  $U$  for the case

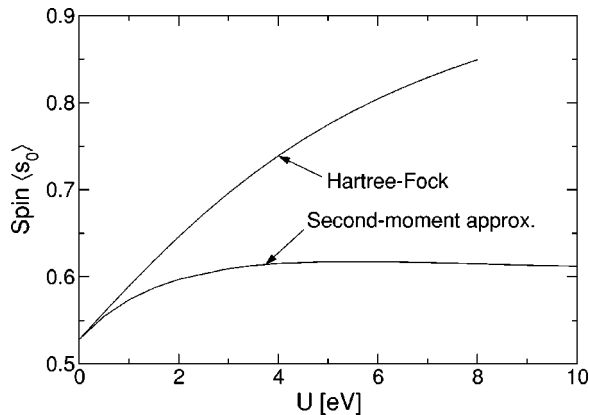


FIG. 4. Spin of the dangling-bond orbital as a function of interaction energy  $U$  for the case that the chemical potential lies between the two defect levels. The spin is measured in units of the electron spin.

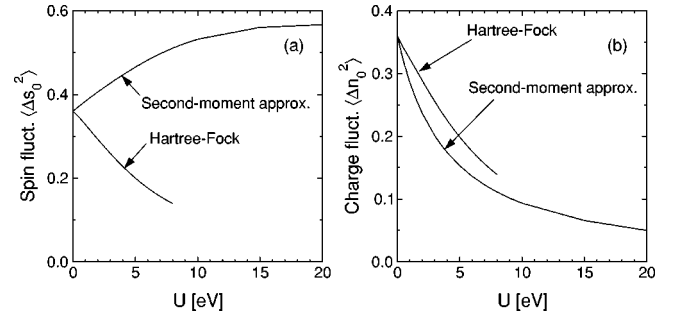


FIG. 5. Fluctuations of the spin (a) and the charge (b) on the dangling-bond orbital as a function of the interaction energy  $U$ .

when the chemical potential is between the two defect levels. In the second-moment approximation, the spin rises for small values of  $U$  and then levels off at a value about 15% higher than the zero- $U$  value. In contrast, the spin in the UHF approximation continues to rise at the highest values of  $U$  that were treated, and eventually approaches unity. This is analogous to the behavior observed for Anderson-chain models.<sup>12</sup> In these models, the UHF approximation overestimates the local moment on the dangling-bond site in order to reduce the interaction energy. The second-moment approximation, however, does not yield such a large local moment. The reason is that in the second-moment approximation correlations are included via multiconfiguration effects, rather than by varying the moment of a single configuration.

The fluctuations in the spin and charge are also obtained straightforwardly by the density-matrix approach. To accomplish this, we note that Eq. (2) implies that  $E_{\text{int}}/U = \langle n_{0\uparrow} n_{0\downarrow} \rangle$ . Then the spin and charge fluctuations on site 0 are obtained as

$$\begin{aligned} \langle (\Delta s_0)^2 \rangle &= \langle s_0^2 \rangle - \langle s_0 \rangle^2 \\ &= \langle n_{0\uparrow} + n_{0\downarrow} \rangle - \langle n_{0\uparrow} - n_{0\downarrow} \rangle^2 - 2E_{\text{int}}/U \end{aligned} \quad (6)$$

and

$$\begin{aligned} \langle (\Delta n_0)^2 \rangle &= \langle n_0^2 \rangle - \langle n_0 \rangle^2 \\ &= \langle n_{0\uparrow} + n_{0\downarrow} \rangle - \langle n_{0\uparrow} + n_{0\downarrow} \rangle^2 + 2E_{\text{int}}/U. \end{aligned} \quad (7)$$

Here we have used the fact that  $\langle n_{0\uparrow}^2 \rangle = \langle n_{0\uparrow} \rangle$  and  $\langle n_{0\downarrow}^2 \rangle = \langle n_{0\downarrow} \rangle$ . The dependence of  $\langle (\Delta s_0)^2 \rangle$  on  $U$  is plotted in Fig. 5(a). In the second-moment approximation, the spin fluctuations increase with  $U$ , to an asymptotic value about 60% higher than the  $U=0$  value. In contrast, the UHF results reveal a monotonic decrease of  $\langle (\Delta s_0)^2 \rangle$  with  $U$ . These results are consistent with the Anderson-chain results.<sup>12</sup> The decrease in the spin fluctuation with  $U$  in the UHF approximation results from the increased moment obtained in this approximation, while the increase observed in the second-moment approximation results from the reduced occupancy of the zero-spin states in which both orbitals on site 0 are empty or filled. The charge fluctuations on site 0 are shown in Fig. 5(b). In both the second-moment and UHF approximations, the fluctuations drop with increasing  $U$ . However, the second-moment approximation yields a more pronounced drop than the UHF approximation. The behavior of the



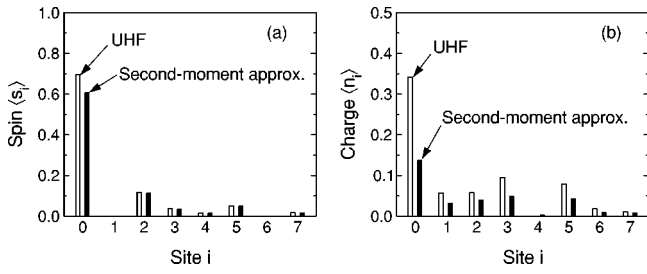


FIG. 6. Spin and charge density of the defect state projected on the chain sites for  $U=3$  eV. Correlation effects as described by the second-moment approximation delocalize the charge of the defect state but not the spin.

charge fluctuations, like that of the spin fluctuations, is due to the suppression of configurations with zero or double occupancy with increasing  $U$ .

#### D. Comparison to experiments and previous theory

The primary outputs of these calculations that can be compared with experiment and previous theory are the spin and charge localization of the gap states, and their splitting. We expect the electronic structure of gap states in  $a$ -Si:H to be described qualitatively by the present model. A quantitative comparison to experimental data is difficult since the strength of the bare Coulomb interaction,  $U$ , for dangling bonds in amorphous silicon is not known precisely, and we ignore relaxation processes, which are known to reduce the effective correlation energy.<sup>19</sup>

The most reliable value of  $U$  for this system comes from a fit to experimental surface state splittings<sup>19</sup> using an accurate electronic-structure model, which yields  $U=4$  eV. We note that expansion of the interaction term in Eq. (1) of Ref. 19 gives a definition of  $U$  equivalent to that used here. A simple electrostatic estimate gives  $U=1$  eV.<sup>20</sup> Other calculations involving  $U$  for amorphous Si have either used that from Ref. 19, given values without justification, or used highly simplified electronic-structure models.<sup>3,21,22</sup> For this reason we take  $U$  to be 4 eV.

Figure 6(a) shows the charge density of the defect state projected on the sites of the recursion chain for the second-moment approximation and the UHF approximation. The components of the gap-state charge density on the sites other than 0 are found by evaluating the changes in site-projected charges when the chemical potential crosses up through the lower gap level. For the comparison we use a slightly smaller value of  $U=3$  eV since beyond this value of  $U$  the defect states are no longer in the gap in the UHF approximation. The differences between the two methods would be even larger at  $U=4$  eV. The neglect of the correlation effects in the UHF approximation results in an overestimate of the charge localization of the defect state on the dangling bond orbital. In the second-moment approximation, the charge is strongly delocalized over a large part of the chain. The spin, on the other hand, is strongly localized on the dangling bond orbital. The UHF yields a slightly larger spin than the second-moment approximation. Overall, the correlation ef-

TABLE I. Comparison of the splitting  $\Delta\epsilon$  of the defect state in the energy gap as well as the spin and charge localization from different methods to experimental values. The projected spin  $\langle s_{db} \rangle$  and charge  $\langle n_{db} \rangle$  of the defect onto the four  $sp^3$  orbitals of the atom associated with the dangling bond are given in units of the electron spin and charge, respectively.

	$\Delta\epsilon$ [eV]	$\langle s_{db} \rangle$	$\langle n_{db} \rangle$
LDA <sup>8</sup>	—	—	0.10–0.15
LSDA <sup>11</sup>	0.25–0.30	0.41–0.52	0.16
UHF	0.9	0.70	0.40
Second-moment approximation	0.5	0.62	0.12
Experiment	0.3–0.4 <sup>23,24</sup>	0.50–0.80 <sup>9,10</sup>	—

fects lead to a larger degree of localization for the spin than for the charge. This confirms the LSDA results by Fedders *et al.*<sup>11</sup>

For  $U=4$  eV, the gap state splitting is already close to its asymptotic large- $U$  value, which is determined by the coupling of the gap state to the neighboring orbitals. Table I compares the gap state splitting as well as the spin and charge localization of the defect state to experimental data and previous density-functional results in Table I. For completeness the UHF are also included in the comparison for a value of  $U=3$  eV.

ESR and photoluminescence spectroscopy measurements have given values for the splitting of the two gap states ranging from 0.3 to 0.4 eV.<sup>23,24</sup> These splittings are close to those obtained here for a wide range of values of  $U$ . Comparable agreement is obtained by the LSDA calculations, but the UHF method overestimates the splittings. The extent of spin localization in the present results is very insensitive to  $U$ , and is roughly in the middle of the range obtained in ESR experiments.<sup>1,9,10</sup> Again, the LSDA results are quite comparable. In both approaches, the degree of spin localization of the defect state on the dangling bond is much greater than the localization of the charge; however, this does not hold for the UHF results. Overall, the agreement of the results of the second-moment approximation with experimental values is surprisingly good, considering the simplicity of the underlying tight-binding model. To our knowledge, no experimental methods exist for measuring the extent of charge localization on the dangling-bond orbital.

#### V. CONCLUSION

The above results illustrate the applicability of the second-moment implementation of density-matrix functional theory to electronic-structure models with semiquantitative accuracy such as the tight-binding model used here. The results show that the splitting of the gap states is smaller than expected from Hartree-Fock calculations and approaches a finite limit for large values of the Coulomb repulsion. This effect can be explained by the enhanced correlation of the electrons in dangling-bond states with increased Coulomb repulsion. It is found that the spin of the defect state is strongly localized on the dangling bond orbital while the charge is quite delocalized. These results are rather insensi-

tive to the specific value of the Coulomb repulsion parameter, and are in fairly good agreement with results from electron spin resonance experiments and local-spin density functional calculations. Our results for the charge fluctuations are similar to those obtained from Hartree-Fock theory, while the results for spin fluctuations are quite distinct. We are not aware of existing methodologies for measuring these fluctuations, but such measurements could provide an accurate test of the precision of the methods used here.

Because of the previously demonstrated<sup>12</sup> applicability of the second-moment implementation of density-matrix functional theory to strongly interacting systems, it would be de-

sirable to apply it to transition-metal impurities in both semiconductors and insulators. At this point, such applications cannot be performed because we do not have a suitable energy functional for such a multiorbital impurity. Future work in this field should aim to extend the present methodology to include such systems with more than two interacting orbitals.

#### ACKNOWLEDGMENTS

This work was supported by NSF Grant No. DMR-9971476.

---

\*Current address: Department of Physics, The Ohio State University, Columbus, OH 43210.

<sup>1</sup>R.A. Street, *Hydrogenated Amorphous Silicon* (Cambridge U.P., New York, 1991).

<sup>2</sup>D.C. Allan and E.J. Mele, Phys. Rev. B **31**, 5565 (1985).

<sup>3</sup>R. Biswas, C.Z. Wang, C.T. Chan, K.M. Ho, and C.M. Soukoulis, Phys. Rev. Lett. **63**, 1491 (1989).

<sup>4</sup>P.A. Fedders and A.E. Carlsson, Phys. Rev. B **39**, 1134 (1989).

<sup>5</sup>J. Holender and G. Morgan, J. Phys.: Condens. Matter **4**, 4473 (1992).

<sup>6</sup>S. Knief and W. von Niessen, Phys. Rev. B **58**, 4459 (1998).

<sup>7</sup>B.J. Min, Y.H. Lee, C.Z. Wang, C.T. Chan, and K.M. Ho, Phys. Rev. B **45**, 6839 (1992).

<sup>8</sup>P.A. Fedders and D.A. Drabold, Phys. Rev. B **47**, 13277 (1993).

<sup>9</sup>D.K. Biegelsen and M. Stutzmann, Phys. Rev. B **33**, 3006 (1986).

<sup>10</sup>T. Umeda, S. Yamasaki, J. Isoya, and K. Tanaka, Phys. Rev. B **59**, 4849 (1999).

<sup>11</sup>P.A. Fedders, D.A. Drabold, P. Ordejon, G. Fabricius, D.

Sanchez-Portal, E. Artacho, and J.M. Soler, Phys. Rev. B **60**, 10594 (1999).

<sup>12</sup>R.G. Hennig and A.E. Carlsson, Phys. Rev. B **63**, 115116 (2001).

<sup>13</sup>P.A. Fedders, Phys. Rev. B **64**, 165206 (2001).

<sup>14</sup>J.C. Slater and G.F. Koster, Phys. Rev. **94**, 1498 (1954).

<sup>15</sup>M. Levy, Proc. Natl. Acad. Sci. U.S.A. **76**, 6062 (1979).

<sup>16</sup>W.A. Harrison, *Electronic Structure and the Properties of Solids* (Dover, New York, 1989).

<sup>17</sup>R. Haydock, Solid State Phys. **35**, 215 (1980).

<sup>18</sup>R.G. Hennig, Ph.D. thesis, Washington University in St. Louis, 2000.

<sup>19</sup>O.L. Alerhand and E.J. Mele, Phys. Rev. Lett. **59**, 657 (1987).

<sup>20</sup>J.E. Northrup, Phys. Rev. B **40**, 5875 (1989).

<sup>21</sup>D. Tomanek and M.A. Schluter, Phys. Rev. B **36**, 1208 (1987).

<sup>22</sup>T. Koslowski, S. Knief, and W. von Niessen, Phys. Rev. B **54**, 13420 (1996).

<sup>23</sup>D. Jousse, Appl. Phys. Lett. **49**, 1438 (1986).

<sup>24</sup>J.-K. Lee and E.A. Schiff, Phys. Rev. Lett. **68**, 2972 (1992).